

PROCEEDINGS OF SPIE

[SPIDigitalLibrary.org/conference-proceedings-of-spie](https://spiedigitallibrary.org/conference-proceedings-of-spie)

Vertical travelling scatterometry for metrology on fully integrated devices

Schmidt, D., Medikonda, M., Rizzolo, M., Silvestre, C., Frougier, J., et al.

D. Schmidt, M. Medikonda, M. Rizzolo, C. Silvestre, J. Frougier, A. Greene, M. Breton, A. Cepler, J. Ofek, I. Kaplan, R. Koret, I. Turovets, "Vertical travelling scatterometry for metrology on fully integrated devices," Proc. SPIE 12053, Metrology, Inspection, and Process Control XXXVI, 120530S (26 May 2022); doi: 10.1117/12.2614077

SPIE.

Event: SPIE Advanced Lithography + Patterning, 2022, San Jose, California, United States

Vertical Travelling Scatterometry for Metrology on Fully Integrated Devices

D. Schmidt^{a,*}, M. Medikonda^a, M. Rizzolo^a, C. Silvestre^a, J. Frougier^a, A. Greene^a, M. Breton^a,
A. Cepler^b, J. Ofek^c, I. Kaplan^c, R. Koret^c, I. Turovets^c

^aIBM Research, 257 Fuller Road, Albany, NY, USA 12203

^bNova Measuring Instruments Inc, 3342 Gateway Blvd, Fremont, CA, USA 93117

^cNova Ltd, 5 David Fikes St, Rehovot, Israel 7610201

*schmidt@ibm.com

ABSTRACT

In this work, a novel spectral interferometry technique called vertical travelling scatterometry (VTS) is introduced, demonstrated, and discussed. VTS utilizes unique information from spectral interferometry and enables solutions for applications that are infeasible with traditional scatterometry approaches. The technique allows for data filtering related to spectral information from buried layers, which can then be ignored in the optical model. Therefore, using VTS, selective measurements of the topmost part of an arbitrarily complex stack are possible within a single metrology step. This methodology helps to overcome geometrical complexities and allows focusing on parameters of interest through dramatically simplified optical modelling. Such model simplifications are specifically desired for back-end-of-line applications. Three examples are discussed in this paper: monitoring (i) critical dimensions of a first metal level on top of nanosheet gate-all-around transistor structures, (ii) the thickness of an interlayer dielectric above embedded memory in the active area, and (iii) critical dimensions of trenches on top of tall stacks in the micrometer range comprising many layered dielectrics. It was found that, in all three cases, data filtering through VTS allowed for a simple optical model capable of delivering parameters of interest. The validity and accuracy of the VTS solution results were confirmed by extensive reference metrology obtained by traditional scatterometry, scanning electron microscopy, and transmission electron microscopy.

Keywords: Vertical Travelling Scatterometry, Scatterometry, OCD, Spectral Reflectometry, Spectral Interferometry

1. INTRODUCTION

Due to the ever-shrinking dimensions of semiconductor devices, there is a constant drive for in-die and fully integrated device metrology to capture subtle differences where they matter rather than going through a dedicated metrology target in the scribe line. More importantly, scribe line targets usually comprise simplified stacks and designs to focus on a specific process step of interest and to not be impacted by prior process variations where possible. These simplifications may result in minor structural differences compared to fully integrated device stacks, and they are starting to matter more with shrinking dimensions. Furthermore, the recent developments of embedding memory elements in the early back-end-of-line (BEOL) of the manufacturing process demand advanced materials and dimensional metrology very late in the process previously not required.¹ In particular, there is now a significant need for optical critical dimension (OCD) metrology during these later stages of device manufacturing.² The most advanced back-end memory devices are embedded between the first and second metal level on top of front-end CMOS logic. The integration scheme requires a dielectric chemical-mechanical polishing (CMP) planarization that necessitates in-line monitoring on the active device for tight process control. This results in substantial modeling challenges due to the large number of layers and buried three-dimensional features and front-end architecture. The cumulative statistical process variations would all need to be considered for an accurate optical model leading to a large number of floating parameters. Depending on the stack complexity, traditional OCD approaches may not be capable of solving these tasks anymore with the required precision for the parameters of interest.

Recently, OCD was enhanced with spectral interferometry technology by providing absolute phase information to improve sensitivity to weak target parameters and reducing parameter correlations.³ In this paper, a novel way of using spectral

interferometry is introduced, which enables OCD to overcome geometrical complexities and allows focusing on the parameters of interest. The new technique, called vertical traveling scatterometry (VTS), allows for a selective measurement of the top part of a stack separately from the bottom part within a single metrology step only. Thus, VTS solutions can simply exclude any complex or unknown underlayers, which allows for solving applications that are not feasible with traditional scatterometry approaches. This paper demonstrates VTS capabilities for three different BEOL examples: (i) measuring critical dimensions (CDs) of a first metal level on top of nanosheet gate-all-around transistor structures,^{4,5} (ii) measuring the thickness of an interlayer dielectric above embedded memory in the active area¹ and (iii) measuring CDs of trenches on top of tall stacks in the micrometer range comprising many layered dielectrics. All VTS results are validated with traditional OCD, scanning electron microscopy (SEM), or transmission electron microscopy (TEM).

2. BEOL SCATTEROMETRY CHALLENGES AND STRATEGIES

With the continued pitch scaling, also enabled through the insertion of EUV lithography, CD metrology in the BEOL gains even more importance. Because of the decreasing dimensions, seemingly small differences between metrology proxy targets typically found in the scribe line and in the active areas may play an important role for overall device performance. Therefore, in-die measurements are desired, or, at least measurements on proxy targets that mimic the device stack as close as possible. However, tall stacks with buried complex architectures are very challenging for model-based metrology techniques such as scatterometry.

Typically, OCD developments for logic devices are reported for wafers with BEOL short-loop processing, i.e. no front-end-of-line (FEOL) or middle-of-line (MOL) content is present.⁶⁻¹⁰ Transferring these learnings to manufacturing is not always straightforward because of the aforementioned challenges. Timoney et al. are discussing the substantial modelling complexities for M2 on fully integrated targets at the 7 nm and 14 nm node.¹¹ The incoming process variations can impact the measurement uncertainty and may lead to a significant measurement error of the features of interest. The authors propose a hybrid modelling technique (combining OCD with another measurement technique) to mitigate some of the uncertainties but details are omitted.

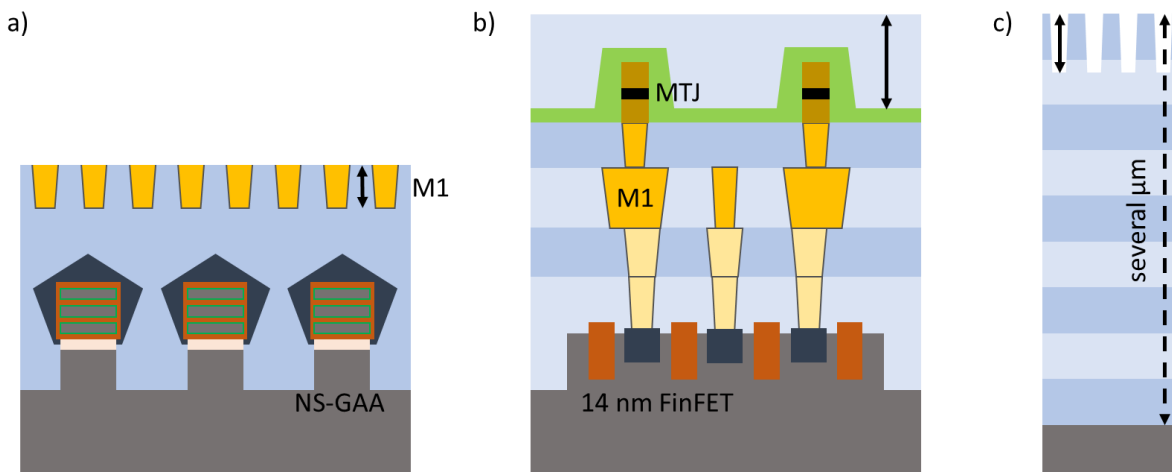


Figure 1. Schematics of challenging BEOL scenarios for traditional scatterometry. (a) critical dimensions of the M1 metal level on top of nanosheet gate-all-around (NS-GAA) transistor structures, (b) the thickness of the topmost interlayer dielectric above embedded memory in the active area and (c) critical dimensions of trenches on top of tall stacks in the micrometer range comprising many layered dielectrics.

Figure 1 illustrates three typical BEOL scenarios that pose significant challenges for traditional scatterometry and may render an optical model infeasible. Measuring the line height and CDs of the first metal layer (M1) on top of a nanosheet gate-all-around (NS-GAA) device architecture using OCD is very challenging (Figure 1a).^{4,5} Even though in this example,

the metrology target does not comprise MOL contacts, an optical model would require many degrees of freedom to account for statistical process variations associated with the nanosheets including gate stack and source/drain region, for example. Furthermore, in case of any FEOL process changes, a model would likely require a significant update and re-optimization leading to a long time-to-solution. Figure 1b depicts an example of MRAM embedded between M1 and M2. Besides CD measurements of the magnetic tunnel junction (MTJ) and its electrodes, the interlayer dielectric (ILD) thickness must be monitored also in the active region (on device). The integration scheme requires planarization before M2 patterning and the CMP process homogeneity across the chip is critical to prevent subsequent processing issues.¹ A traditional optical model for the active area is infeasible because the OCD spectra carry information from the entire device architecture including FEOL and wiring all the way to the memory pillar and ILD. The last example of a trenches at the top of a tall stack comprising many layers of optically transparent dielectrics may appear like a simple one (Figure 1c). However, once the total stack thickness reaches several micrometers the measured OCD spectra are dominated by strong oscillations due to thin film interference effects related to the tall stack and the many layer interfaces. A traditional OCD solution would be extremely cumbersome and sensitivity to the critical parameters of interest likely still low.

There are several pathways to a solution for the discussed scenarios, but they are coming with numerous disadvantages. While a feedforward or hybrid model does reduce the number of degrees of freedom, it still requires a complex geometric optical model including data from either previous or other measurement steps.^{8,9,11,12} Another variation of hybrid metrology is related to “differential modeling”, which requires measurements before and after the process step of interest along with appropriate algorithms.¹³ There are certain constraints, and the methodology does not necessary simplify the solution.

Machine learning can enable scatterometry solutions without the need for a geometrical model and may even allow prediction of parameters inaccessible with traditional model solutions.^{9,10,14,15} However, the required reference data is not always easy to obtain. It may also be very time consuming and expensive if, for example, only cross-sectional TEM reference metrology is an option. Interestingly, in the case of tall stacks (Figure 1c), a very large reference data set would be required for a successful machine learning model because the measured optical spectra contain the convolution of parameters of interest related to the trenches and information of each buried layer.

If measurements can be performed on specifically designed targets in the scribe line, design modifications can help to engineer the optical response such that the solution may be simplified. In the case of tall stacks with many transparent dielectric layers, it may be helpful to introduce buried patterned metal layers if the process flow allows. These can help to suppress contributions in the optical response from layers below, thereby reducing interference fringes and limiting sensitivity to buried layers. Materials, critical dimensions, volume, number of patterned layers and orientation must be considered during the design phase to achieve desired simplifications. Of course, the patterned layers must then be considered in the final optical model.

In all described scenarios, the root cause of the BEOL modelling complexities is the fact that the measured optical spectra contain information from the entire stack. Hence, the irrelevant information of all buried layers and architectures is convoluted with the optical response from the topmost features of interest. A deconvolution is desired to separate relevant from irrelevant information and thus to substantially increase sensitivity to the parameters of interest, and to dramatically simplify the optical solution.

3. VERTICAL TRAVELLING SCATTEROMETRY (VTS)

Vertical travelling scatterometry (VTS) uses unique information from spectral interferometry along with novel algorithms to enable a deconvolution of spectral information relative to the depth from which they are originating. Hence, it allows for a separation of relevant and irrelevant optical information thereby enabling selective measurements of the topmost layers of interest within a single metrology step. The algorithm allows for filtering of data obtained through spectral interferometry channels such that the dominant part of the information from below the cut-off can be selectively removed from the measured optical response (Figure 2). Hence, underlayer contributions may be ignored, which can dramatically reduce the geometrical complexities and significantly increases the sensitivity to parameters of interest. Additionally, the simplified optical model improves the time-to-solution. The utilization of VTS allows for solving applications that are otherwise not feasible with traditional scatterometry approaches. Because of the filter cut-off and the ability to ignore spectral information, the same optical model can be use regardless of the type of underlayers (solid or patterned) and its process variations. Figure 3 depicts an example of two tall stacks with a total thickness of 4.5 μm that have a difference in one of the underlayers (patterned Cu lines introduced in one of the stacks) but otherwise identical trench patterning (top

of the stack). The simulated spectral interference spectra for four different channels within the UV to NIR range are dominated by strong oscillations related to thin film interference effects. It is evident that the original spectra are different because of the variation in one of the buried layers (Figure 3c,e). Applying a VTS filter removes the dominant part of the underlayer signals and hence substantially reduces the oscillations (Figure 3d,f). When using the filtered VTS spectra, a simplified optical model can be employed that does not need to account for underlayer contributions and allows focusing on the desired trench characterization.

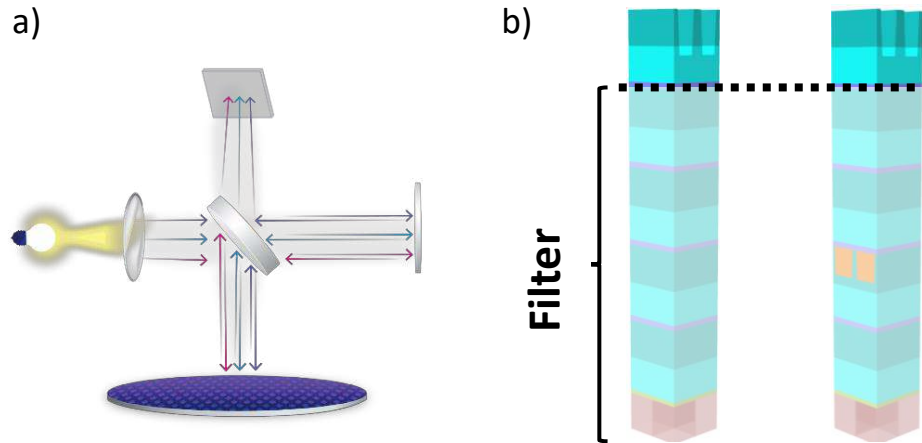


Figure 2. (a) Schematic of a spectral interferometer: white light is split between the sample and a reference arm and then recombined and measured with a spectrometer. (b) Illustration of VTS filtering where spectral information from below the cut-off (dashed line) can be identified and removed from the optical response.

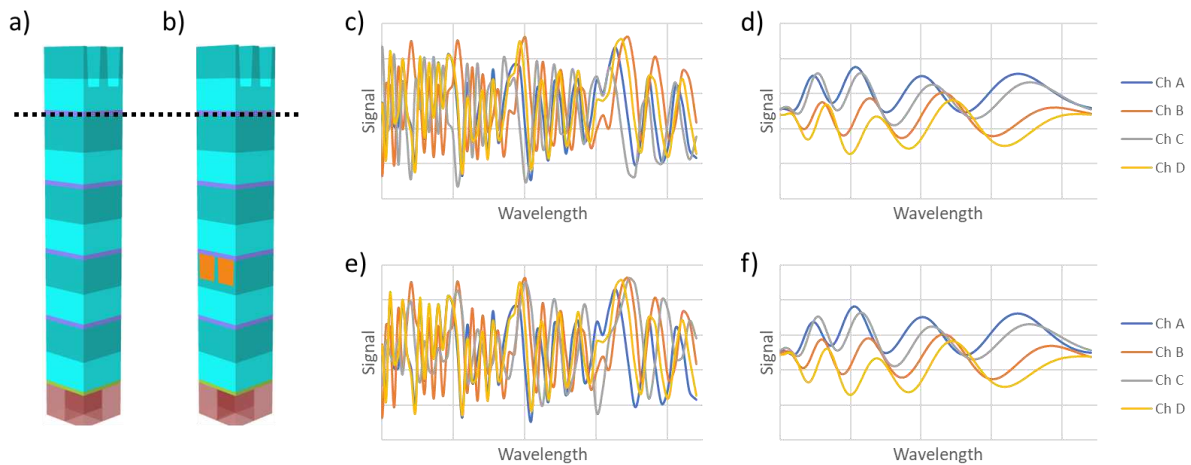


Figure 3. Comparison of tall stacks ($4.5\ \mu\text{m}$ total thickness) with a) only solid dielectric and b) solid dielectric and a patterned Cu underlayers. (c,e) Original spectral interferometry channels and (d,f) VTS filtered spectra where the (c,d) top and (e,f) bottom rows show simulated graphs for stacks (a) and (b), respectively. The dashed lined indicates the VTS filter cut-off position. Each graph shows a total of four different, polarization-dependent channels (Ch A through Ch D). Both axes are identical for each of the four graphs.

4. APPLICATION EXAMPLES

4.1 BEOL Trenches on Tall Stacks

In order to verify VTS for tall stacks, the selected application requires monitoring trench height and CD for the fifth metal layer of a short-loop BEOL flow. For the specific metrology target under investigation, all layers below the trenches of interest are not patterned and comprise only thin films of various BEOL dielectrics, which are optically transparent. The total stack thickness measured from the substrate interface is approximately 4.5 μm . As discussed above, the collected OCD spectra are overwhelmingly dominated by oscillations but through spectral filtering, the optical model can be reduced to the topmost part of the stack (above the filter) comprising the trenches. Four wafers with dose variations were exposed to intentionally change the trench CD: three wafers with fixed dose values and one wafer with a dose stripe (variable dose across the wafer). After collection of the optical spectra, top-down CDSEM reference data were obtained from twelve dies per wafer. On a different set of five wafers, a trench height variation was achieved through etch time differences. For wafers 1 and 3 an increased and decreased etch time was used, respectively. The other three wafers were etched at nominal conditions. To verify the trench depth, cross-sectional SEM reference data was obtained for two dies from each of the five wafers. A schematic of the stack and the VTS results in comparison to reference metrology are shown in Figure 4. The VTS solution results show very good correlation to the reference metrology, particularly for trench height. These results confirm the basic working principle of VTS and verify that it is possible to filter irrelevant spectral information from buried layers. This methodology can also be very beneficial for machine learning based solutions. Training a model with VTS filtered spectra will require only a reduced reference data set with variations of the parameters of interest. In contrast, training a comparable machine learning model with unfiltered, original spectra will require a much larger reference set comprising additionally process variations of all underlayers.

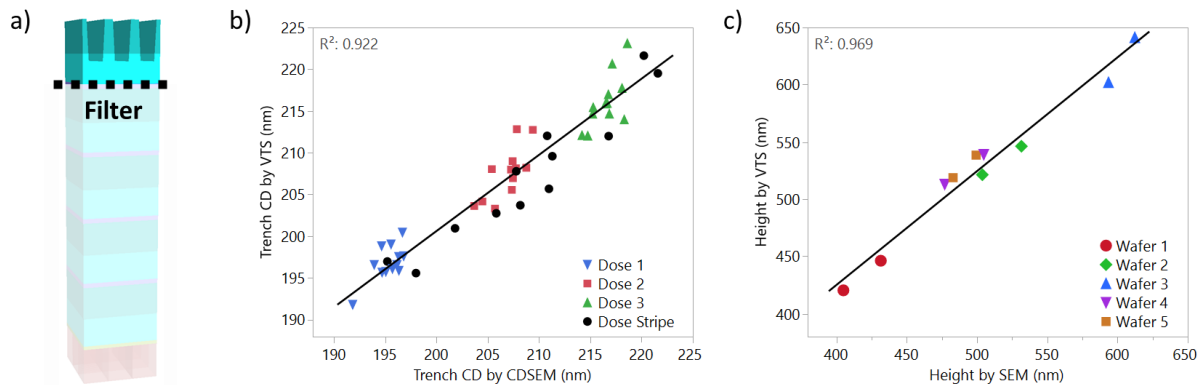


Figure 4. a) Schematic of stack including VTS filter and comparison between reference metrology and VTS results for b) trench CD and c) trench height. The trench CD reference was obtained by CDSEM and the trench height by cross-sectional SEM.

4.2 M2 ILD CMP on Fully Integrated Embedded MRAM Devices

Embedding memory elements in the early BEOL requires a dielectric planarization before the subsequent metal patterning since the MRAM pillars introduce topography otherwise not present. The ILD thickness is location- and design-dependent, and process variations may lead to metallization defects. In the particular case discussed here, measuring a proxy target in the scribe line is not sufficient to detect process excursion and thickness monitoring on fully integrated devices post CMP is required. The MRAM elements are embedded between M1 and M2 on top of a fully build CMOS architecture. A traditional OCD approach would be extremely challenging due to the optical model complexities, if at all possible. The many degrees of freedom required to account for statistical process variations very likely would lead to a large measurement uncertainty not sufficient to control the process.

Four wafers with different CMP split conditions but otherwise identical processing were manufactured. Spectra for both dedicated metrology targets in the scribe line (MTJ only) and fully integrated devices in the active area (MTJ + CMOS) were collected post ILD CMP on all wafers (Figure 5). Both targets comprise MRAM pillars with identical dimensions

and the difference between the scribe line targets and the active area was merely the patterning below the memory elements. Specifically, the MTJ-only targets do not comprise any patterned features below the memory pillar but only several thin films (Figure 5a). Figure 5b shows the distinct differences in ILD height after CMP between the two target areas. Moreover, different CMP process conditions do not lead to a constant offset between the two measured targets, which is the main reason why in-die measurements are key for successful in-line process monitoring.

A geometric optical model was built to analyze the dedicated MTJ only metrology target. Using rigorous coupled wave analysis (RCWA) algorithms it is possible to solve for the total ILD thickness and the remaining ILD thickness above the pillar. Due to the above discussed structural complexities, a geometric optical model was not attempted for the measured in-die active area. Rather, VTS was used to filter the measured spectra from the fully integrated area such that the irrelevant spectral information from the buried CMOS does not need to be considered. Consequently, the optical model can be dramatically simplified. This VTS solution was then used to analyze measured spectra from both targets: MTJ only and MTJ + CMOS. The excellent match of VTS results to reference metrology is shown in Figure 5c. For the MTJ only target, the ILD height as a result of the traditional OCD model serves as reference. Note that here the remaining ILD thickness above the pillar is plotted rather than the height in the open areas. A total of twelve cross-section TEM images from the MTJ + CMOS targets were analyzed to obtain the total ILD thickness in the area between the pillars for all four CMP conditions. These results confirm that the VTS algorithm can be used to analyze fully integrated targets to obtain device information where a traditional model is infeasible. Moreover, it is possible to use the same VTS solution for analyzing different target types.

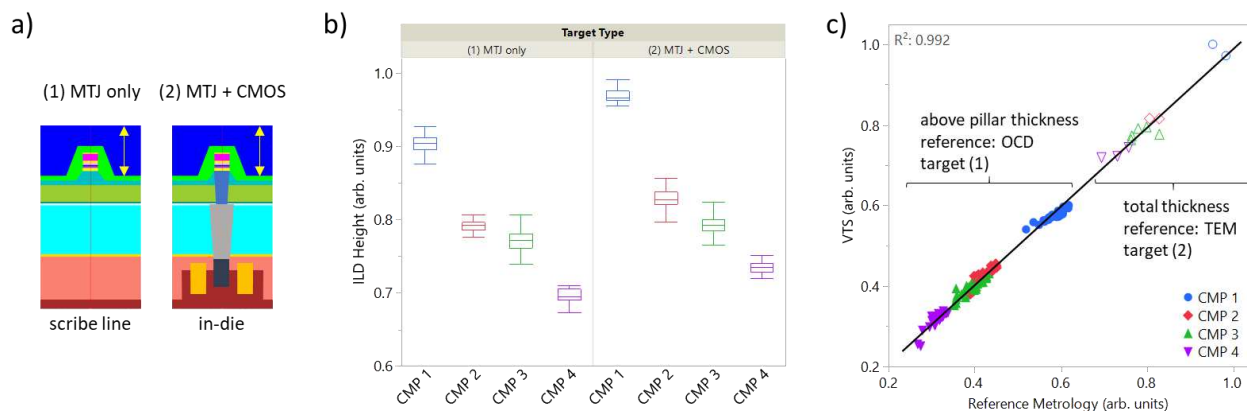


Figure 5. (a) Schematics of dedicated MRAM metrology target in the scribe line and active device (in-die) comprising MRAM pillars on top of a 14 nm CMOS node. (b) ILD height box plot with across wafer data for both targets as a function of four different CMP split conditions. (c) Correlation between VTS results and reference measurements from all four split conditions. The open symbols correspond to TEM and the solid symbols to OCD reference data, respectively.

4.3 M1 CMP on Integrated Nanosheet Gate-All-Around Devices

For early BEOL applications such as M1, there is a desire to measure critical dimensional parameters using OCD on targets that are device-like or with little simplifications to match device processing closely rather than on targets that skip FEOL patterning altogether. Subtle metal line height differences that may be observed after CMP related to microtopography, for example, do not have to be considered and characterized when measuring and monitoring on device-like targets. Often, this is not done though because of the inherent model complexities and the increased measurement uncertainty that then outweigh the benefits significantly. Or often cumbersome hybrid model techniques have to be developed to lower measurement uncertainties but still require a detailed and complicated geometric optical model. Specifically in the process development stage, an OCD solution comprising a full optical model is usually not a preferred path. Continuous process improvements in the FEOL and MOL would require frequent updates of the optical model, which is not economical due to the long time-to-solution. VTS enables monitoring of M1 CDs on top of a full FEOL build comprising nanosheet gate-all-around architectures without the need to consider or model any of the FEOL features, for example. Figure 6a depicts a cross-sectional TEM image of a dedicated metrology target comprising nanosheets including gate and source drain (MOL

contacts are omitted here). VTS can be used to filter the spectral information related to the FEOL and allows focusing on the M1 characteristics only. The results of the VTS solution show a very good correlation to OCD and cross-sectional TEM reference metrology (Figure 6). Note that a traditional OCD model was not developed for the device-like target containing M1 and NS-GAA FEOL due to the architectural complexity. For simplicity and to avoid a time-consuming model solution, the depicted VTS to OCD comparison is using results from a short-loop BEOL wafer with only M1 patterning. The TEM results are obtained from full-flow wafers and the targets comprising M1 on top of a full FEOL build with NS-GAA features (Figure 6a) as well as targets comprising patterned M1 only (Figure 7b), respectively. For all three measured scenarios (short-loop M1 only, full flow M1 only, and M1 + NS-GAA) the same VTS model was used.

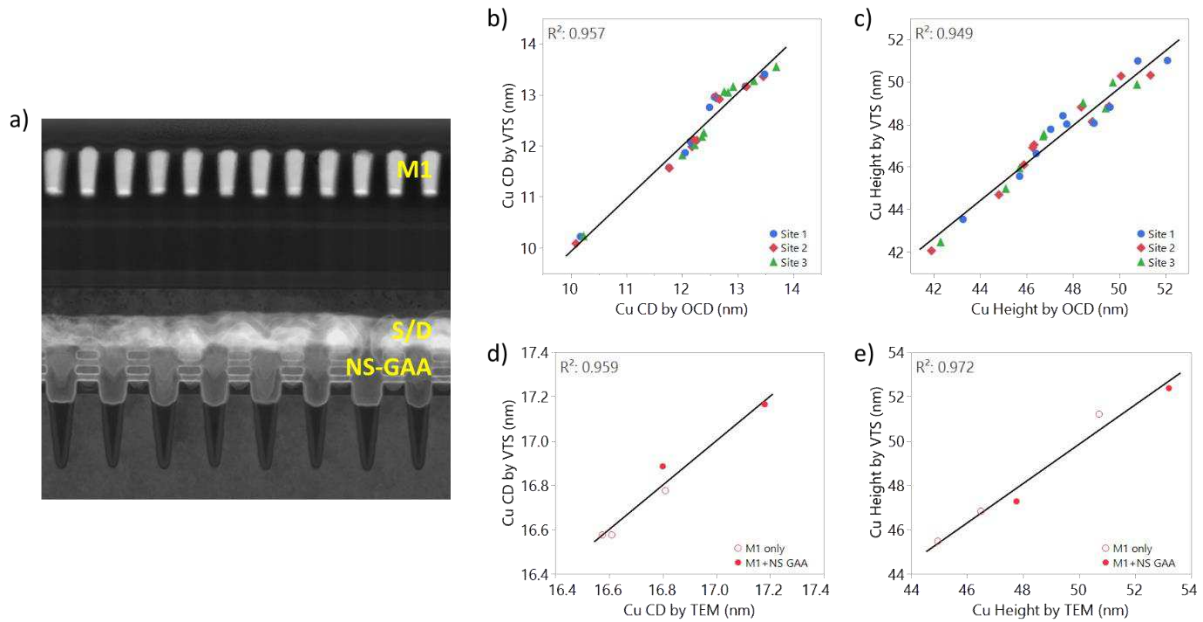


Figure 6. (a) TEM cross-section of a device-like metrology target comprising M1 on top of a full FEOL build with NS-GAA features including gate stack and source/drain; MOL contacts are omitted. (b) M1 Cu CD and (c) M1 Cu height determined by VTS in comparison to OCD reference metrology for three sites and ten measurements each. (d) M1 Cu CD and (e) M1 Cu height determined by VTS in comparison to TEM reference metrology. Open symbols are referring to data from a target having only M1 patterning and solid symbols depict values obtained from a target depicted in (a).

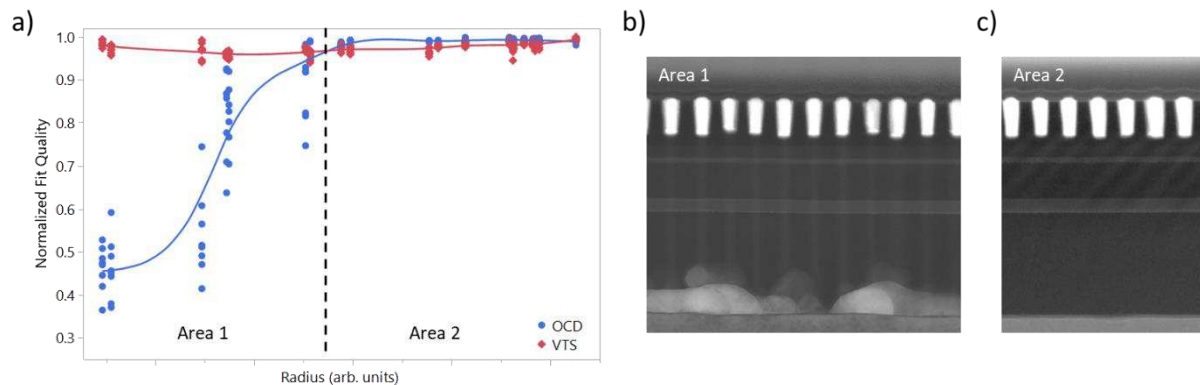


Figure 7. (a) Normalized fit quality obtained from OCD and VTS solutions for a dedicated metrology target comprising M1 patterning only. The cross-section images correspond to areas (b) toward to the center of the wafer (Area 1) and (c) toward the edge of the wafer (Area 2).

While analyzing the dedicated metrology targets with M1 patterning only on some experimental wafers, an interesting observation was made. As expected, the VTS solution delivered consistently good results for all sampled target locations across the wafer. However, the OCD solution fit quality degraded significantly toward the center of the wafer (Figure 7). Cross-sectional TEM images from two representative locations revealed that in Area 1 (toward the center of the wafer) defects are present at the substrate interface. The traditional OCD model, utilizing the full spectral information, starts to fail as soon as defects are present in the probed region. The VTS solution however uses filtered spectral content and is therefore only sensitive to the topmost layers including the M1 layer of interest. Hence, VTS is agnostic to the defects and can deliver equally good results across the entire wafer. This example confirms once again that VTS spectral filtering works as intended and irrelevant spectral information from buried layers can be ignored for a simplified optical solution.

5. CONCLUSIONS

In this paper, vertical travelling scatterometry (VTS) is introduced and demonstrated for three metrology challenges related to state-of-the-art device manufacturing. VTS utilizes information from spectral interferometry and allows for data filtering of irrelevant spectral information from buried layers and features. Therefore, VTS enables selective measurements of the topmost part of a stack, for example, and is agnostic to patterned or blanket underlayer variations. As shown, this can dramatically simplify optical modelling, increase sensitivity to parameters of interest, and decrease time-to-solution significantly. Due to the spectral filtering, applications can be solved with VTS that are not feasible with traditional OCD modeling.

It was shown that VTS can filter out reflections from buried layers and successfully deliver critical dimensional parameters of trenches on top of a tall stack with many dielectric films. Furthermore, M2 ILD CMP monitoring on fully integrated embedded MRAM devices was demonstrated. VTS was used to characterize the remaining ILD thickness in the active area, a task not feasible with traditional OCD modeling that would require a complex geometric model and many floating parameters to account for any process variations. Lastly, an example of M1 monitoring on top of a nanosheet gate-all-around FEOL device architecture was presented. The simplified VTS model is capable of delivering M1 dimensional parameters and it was shown that the relevant metrics can be reported regardless of underlayer variations. The VTS solution is agnostic to the presence of buried defects and thus also to FEOL process variations, meaning the VTS solution does not need to be updated in case of any process changes affecting buried layers or features.

This is not only of high value for process development but also for high-volume manufacturing due to the increase sensitivity to the parameters of interest and the significantly simplified optical model, which leads to a fast time-to-solution. The VTS technique is not only relevant for solving BEOL logic applications but also highly valuable for non-volatile flash memory where tall stacks with many layers have to be measured.

6. ACKNOWLEDGEMENTS

The authors would like to thank Marjorie Cheng, Haibo Liu, Daphna Peimer, Ilya Osherov, Michael Sandler (all Nova), Chih-Chao Yang, Daniel Edelstein, and Nelson Felix (all IBM) for support of this work. Nova acknowledges funding for VTS software development from the Electronic Components and Systems for European Leadership (ECSEL) Joint Undertaking under grant agreement No. 826422.

REFERENCES

- [1] D. Edelstein, M. Rizzolo, D. Sil, A. Dutta, J. DeBrosse, M. Wordeman, A. Arceo, I. C. Chu, J. Demarest, E. R. J. Edwards, E. R. Evarts, J. Fullam, A. Gasasira, G. Hu, M. Iwatake, R. Johnson, V. Katragadda, T. Levin, J. Li, Y. Liu, C. Long, T. Maffitt, S. McDermott, S. Mehta, V. Mehta, D. Metzler, J. Morillo, Y. Nakamura, S. Nguyen, P. Nieves, V. Pai, R. Patlolla, R. Pujari, R. Southwick, T. Standaert, O. van der Straten, H. Wu, C.-C. Yang, D. Houssameddine, J. M. Slaughter, D. C. Worledge, "A 14 nm Embedded STT-MRAM CMOS Technology," 2020 IEEE International Electron Devices Meeting (IEDM), San Francisco, CA, USA (2020); doi: 10.1109/IEDM13553.2020.9371922.

- [2] M. Medikonda, D. Schmidt, M. Rizzolo, M. Breton, A. Dutta, H. Wu, E. R. Evarts, A. Cepler, R. Koret, I. Turovets, D. Edelstein, "Scatterometry based methodologies for characterization of MRAM technology," *Proc. SPIE* **12053**, 12053-41 (2022).
- [3] D. Schmidt, C. Durfee, S. Pancharatnam, M. Medikonda, A. Greene, J. Frougier, A. Cepler, G. Belkin, D. Shafir, R. Koret, R. Shtainman, I. Turovets, S. Wolfling, "OCD enhanced: implementation and validation of spectral interferometry for nanosheet inner spacer indentation," *Proc. SPIE* **11611**, 116111U (2021); doi:10.1117/12.2582364.
- [4] N. Loubet, T. Hook, P. Montanini, C.-W. Yeung, S. Kanakasabapathy, M. Guillom, T. Yamashita, J. Zhang, X. Miao, J. Wang, A. Young, R. Chao, M. Kang, Z. Liu, S. Fan, B. Hamieh, S. Sieg, Y. Mignot, W. Xu, S.-C. Seo, J. Yoo, S. Mochizuki, M. Sankarapandian, O. Kwon, A. Carr, A. Greene, Y. Park, J. Frougier, R. Galatage, R. Bao, J. Shearer, R. Conti, H. Song, D. Lee, D. Kong, Y. Xu, A. Arceo, Z. Bi, P. Xu, R. Muthinti, J. Li, R. Wong, D. Brown, P. Oldiges, R. Robison, J. Arnold, N. Felix, S. Skordas, J. Gaudiello, T. Standaert, H. Jagannathan, D. Corliss, M.-H. Na, A. Knorr, T. Wu, D. Gupta, S. Lian, R. Divakaruni, T. Gow, C. Labelle, S. Lee, V. Paruchuri, H. Bu, M. Khare, "Stacked Nanosheet Gate-All-Around Transistor to Enable Scaling Beyond FinFET," *Symp. VLSI Tech.*, 230–231 (2017); doi: 10.23919/VLSIT.2017.7998183.
- [5] J. Zhang, J. Frougier, A. Greene, X. Miao, L. Yu, R. Vega, P. Montanini, C. Durfee, A. Gaul, S. Pancharatnam, C. Adams, H. Wu, H. Zhou, T. Shen, R. Xie, M. Sankarapandian, J. Wang, K. Watanabe, R. Bao, X. Liu, C. Park, H. Shobha, P. Joseph, D. Kong, A. Arceo De La Pena, J. Li, R. Conti, D. Dechene, N. Loubet, R. Chao, T. Yamashita, R. Robison, V. Basker, K. Zhao, D. Guo, B. Haran, R. Divakaruni, H. Bu, "Full Bottom Dielectric Isolation to Enable Stacked Nanosheet Transistor for Low Power and High Performance Applications," 2019 IEEE International Electron Devices Meeting (IEDM), San Francisco, CA, USA (2019), doi: 10.1109/IEDM19573.2019.8993490.
- [6] L. Towidjaja, C. Raymond, M. Littau, D. Forman, S. G. Hummel, "Back end of line metrology control applications using scatterometry," *Proc. SPIE* **6152**, 61521X (2006); doi: 10.1117/12.656515.
- [7] S. Zangoie, M. Sendelbach, M. Angyal, C. Archie, A. Vaid, I. Matthew, P. Herrera, "Characterization of 32nm node BEOL grating structures using scatterometry," *Proc. SPIE* **6922**, 69220S (2008); doi: 10.1117/12.773088.
- [8] B. L'Herron, R. Chao, K. Kim, W. T. Lee, K. Motoyama, B. Deprospo, T. Standaert, J. Gaudiello, C. Goldberg, "Hybridization of XRF/XPS and scatterometry for Cu CMP process control," *Proc. SPIE* **9424**, 94241M (2015); doi: 10.1117/12.2086155.
- [9] M. Breton, R. Chao, G. R. Muthinti, A. Arceo de la Peña, J. Simon, A. J. Cepler, M. Sendelbach, J. Gaudiello, S. Emans, M. Shifrin, Y. Etzioni, R. Urenski, W. T. Lee, "Electrical test prediction using hybrid metrology and machine learning," *Proc. SPIE* **10145**, 1014504 (2017); doi: 10.1117/12.2261091.
- [10] S. Das, J. Hung, S. Halder, R. Koret, I. Turovets, A.-L. Charley, P. Leray, "Scatterometry solutions for 14nm half-pitch BEOL layers patterned by EUV single exposure," *Proc. SPIE* **11611**, 116112A (2021); doi: 10.1117/12.2583714.
- [11] P. Timoney, A. Vaid, B. C. Kang, H. Liu, P. Isbester, M. Cheng, S. Ng-Emans, N. Yellai, M. Sendelbach, R. Koret, O. Gedalia, "Hybrid scatterometry measurement for BEOL process control," *Proc. SPIE* **10145**, 1014506 (2017); doi: 10.1117/12.2261452.
- [12] A. Vaid, L. Subramany, G. Iddawela, C. Ford, J. Allgair, G. Agrawal, J. Taylor, C. Hartig, B. C. Kang, C. Bozdog, M. Sendelbach, P. Isbester, L. Issascharoff, "Implementation of hybrid metrology at HVM fab for 20nm and beyond," *Proc. SPIE* **8681**, 868103 (2013); doi: 10.1117/12.2012339.
- [13] I. Osherov, L. Issascharoff, O. Gedalia, K. Wakamoto, M. Sendelbach, M. Asano, "Application of advanced hybrid metrology method to nanoimprint lithography," *Proc. SPIE* **10145**, 101451X (2017); doi: 10.1117/12.2266577.
- [14] D. Kong, D. Schmidt, J. Church, C.-C. Liu, M. Breton, C. Murray, E. Miller, L. Meli, J. Sporre, N. Felix, I. Ahsan, A. J. Cepler, M. Cheng, R. Koret, I. Turovets, "Measuring local CD uniformity in EUV vias with scatterometry and machine learning," *Proc. SPIE* **11325**, 113251I (2020); doi: 10.1117/12.2551498.
- [15] D. Schmidt, K. Petrillo, M. Breton, J. Fullam, R. Koret, I. Turovets, A. Cepler, "Advanced EUV Resist Characterization using Scatterometry and Machine Learning," Annual SEMI Advanced Semiconductor Manufacturing Conference (ASMC), Milpitas, CA, USA, (2021), doi: 10.1109/ASMC51741.2021.9435698.